Optical forces on interacting plasmonic nanoparticles in a focused Gaussian beam

Zhipeng Li,[1] Mikael Käll,[2] and Hongxing Xu[1,3,*]

[1]*Beijing National Laboratory for Condensed Matter Physics, Institute of Physics, Chinese Academy of Sciences, Beijing 100080, China*

[2]*Department of Applied Physics, Chalmers University of Technology, SE-412 96 Göteborg, Sweden*

[3]*Division of Solid State Physics, Lund University, P.O. Box 118, Lund S-22100, Sweden*

(Received 4 September 2007; published 8 February 2008)

We theoretically analyze optical forces on aggregates of metal nanoparticles in a focused Gaussian beam by extending the generalized Mie theory, which includes higher order multipoles and retardation effects. For two interacting metallic particles, an attractive gradient force, mainly caused by multipole plasmon excitation, exists at short interparticle distances, while induced dipolar fields dominate for separations of the order of the particle radius R or larger. The long-range force component can be either attractive or repulsive depending on the phase of the induced dipoles, as determined by the illumination wavelength and the collective dipolar plasmon resonance. In particular, the repulsive force that occurs for illumination near the plasmon resonance wavelength can be so large that it overcomes the optical trapping effect of the Gaussian beam.

DOI: 10.1103/PhysRevB.77.085412 PACS number(s): 78.67.Bf, 87.80.Cc, 03.50.De

I. INTRODUCTION

Optical forces acting on small particles can, in general, be divided into two parts: the dissipative force and the gradient force. The dissipative force, which points in the direction of the propagation of the incident light, is caused by the change of momentum of the particle due to reflection and absorption. The gradient force, which is proportional to the intensity gradient of the incident light and caused by the inhomogeneous distribution of the electromagnetic field around the particle, enables optical trapping[1] and manipulation[2] of small particles. However, stable optical trapping relies on the precise balance between the dissipative force and the gradient force, and quantitative evaluation of optical force experiments therefore requires sophisticated electrodynamics theory and simulation.[3] Several methods and approximations have been utilized to calculate the optical forces acting on a single particle in a Gaussian beam, a problem of central importance to laser tweezers technology.[2] Harada and Asakura[4] and Chaumet and Nieto-Vesperinas,[5] for example, used the dipole approximation to investigate the small-particle case, while Ashkin[6] used ray optics to model the case of micron-sized dielectric particles.

During the last few years, a large interest in optical forces in the context of nano-optics and, in particular, plasmonics has developed.[7–11] We have been particularly interested in induced optical forces between nearby plasmonic nanoparticles. The problem of two interacting metal nanoparticles illuminated by a plane wave was studied theoretically by Xu *et al.*[12] and later by Hallock *et al.*[13] These studies indicated that strong forces can be induced even for relatively weak incident field strengths and that the interaction can be repulsive or attractive depending on incident wavelength, polarization, and surface-to-surface separation. An application of such interparticle forces is surface-enhanced Raman scattering (SERS),[14] which typically utilizes the very large electromagnetic field enhancement that occurs in the junctions between nearly touching noble metal nanoparticles.[12,15] We have recently experimentally demonstrated that optical aggregation of Ag nanoparticles leads to a large increase of the SERS signal from adsorbed organic molecules.[16] In particular, we showed that "hot" pairs of Ag particles could be formed through optical manipulation,[17] and we argued that the final dimerization of the particles within the diffraction limited laser focus was due to the aforementioned optical interparticle force. In this paper, we further describe details of the calculation method used in Ref. 17 and present theoretical results on the optical interaction between silver and gold nanoparticles as a function of particle size and illumination wavelength. Our calculation method is based on the generalized Mie thory,[18] which is well suited for investigations of interactions between spherical plasmonic particles[19] and includes both multipolar effects and retardation. To simulate the optical forces and interactions between two particles in a focused laser beam, we first use the Davis formalism[20] to expand a Gaussian beam into a sum of vector spherical harmonics (VSHs) with different orders.[21,22] The self-consistent scattered fields from the particles are then calculated using the order-of-scattering method.[23,24] This procedure yields the total local field at any point in space as a sum of the incident field and the field scattered from all the nanoparticles in the system. The optical force acting on a given nanoparticle is obtained by integrating the Maxwell stress tensor, which is obtained from the local field, over the surface of the nanoparticle.[25]

The paper is arranged as follows: in Sec. II, the theoretical method is introduced. In Sec. III, the optical forces and the optical potentials of two metallic nanoparticles in a focused Gaussian beam are investigated for different incident wavelengths. In Sec. IV, the limitation of this theory is discussed. A short summary is given in Sec. V.

II. THEORETICAL APPROACH

To introduce a z-axis propagating and x-axis polarized Gaussian beam into the Mie theory, we expand the Davis formula[20] into VSHs. The transverse magnetic (TM) and transverse electric (TE) VSHs are defined as follows:

$$N_{nm}^{(j)} = (\hat{r}, \hat{\theta}, \hat{\varphi}) \begin{bmatrix} n(n+1) z_n^{(j)}(kr) \\ \frac{\partial}{\partial r}\{r z_n^{(j)}(kr)\} \frac{\partial}{\partial \theta} \\ \frac{\partial}{\partial r}\{r z_n^{(j)}(kr)\} \frac{1}{\sin\theta} \frac{\partial}{\partial \varphi} \end{bmatrix} \frac{1}{kr} Y_n^m(\theta, \varphi),$$

$$M_{nm}^{(j)} = (\hat{r}, \hat{\theta}, \hat{\varphi}) \begin{bmatrix} 0 \\ \frac{1}{\sin\theta} \frac{\partial}{\partial \varphi} \\ -\frac{\partial}{\partial \theta} \end{bmatrix} z_n^{(j)}(kr) Y_n^m(\theta, \varphi), \quad (1)$$

where $n \in [1, \infty]$ and $m \in [-n, n]$ are the multipole order and the corresponding angular number, respectively, $\hat{r}, \hat{\theta}, \hat{\varphi}$ are the unit vectors in spherical coordinates, k is the absolute value of the wave vector, $z_n^{(j)}$ are the spherical Bessel functions, corresponding to j_n, y_n, $h_n^{(1)}$, $h_n^{(2)}$ for $j=1,2,3,4$, respectively, and $Y_n^m(\theta, \varphi)$ are spherical harmonics defined in terms of the associated Legendre function P_n^m,

$$Y_n^m(\theta, \varphi) = \sqrt{\frac{(2n+1)(n-m)!}{4\pi(n+m)!}} P_n^m(\cos\theta) \exp(\mathrm{i}m\varphi). \quad (2)$$

We adopt the expansion method of Refs. 21 and 22, where the electromagnetic components in spherical coordinates are expressed by the Bromwich scalar potentials U_{TM} and U_{TE} by introducing the Gaussian expansion coefficients $g_{nm,TM}$ and $g_{nm,TE}$. As an example, the φ component of the electric field is

$$E_\varphi = E_{\varphi,TE} + E_{\varphi,TM} = \frac{i\omega\mu}{r} \frac{\partial U_{TE}}{\partial \theta} + \frac{1}{r \sin\theta} \frac{\partial^2 U_{TM}}{\partial r \partial \varphi}, \quad (3)$$

where $\omega = k/(\mu\varepsilon)^{1/2}$ and μ and ε are the permeability and the permittivity of the medium, respectively. The Bromwich scalar potentials for TM and TE waves are [26]

$$U_{TM} = E_0 \sum_{n=1}^{\infty} \sum_{m=-n}^{n} \frac{i^{n-1}(-1)^n}{k} \frac{2n+1}{n(n+1)} g_{nm,TM} r j_n(kr) P_n^{|m|} \times (\cos\theta) \exp(\mathrm{i}m\varphi),$$

$$U_{TE} = H_0 \sum_{n=1}^{\infty} \sum_{m=-n}^{n} \frac{i^{n-1}(-1)^n}{k} \frac{2n+1}{n(n+1)} g_{nm,TE} r j_n(kr) P_n^{|m|} \times (\cos\theta) \exp(\mathrm{i}m\varphi). \quad (4)$$

By inserting Eq. (4) into Eq. (3) the φ component, the electric field can be expressed in terms of TM- and TE-VSHs as follows:

$$E_\varphi = E_0 \sum_{n=1}^{\infty} \sum_{m=-n}^{n} \left[\frac{i^{n-1}(-1)^n(2n+1)}{n(n+1)F_{YP}} g_{nm,TM} N_{nm,\varphi}^{(1)} + \frac{-i^n(-1)^n(2n+1)}{n(n+1)F_{YP}} g_{nm,TE} M_{nm,\varphi}^{(1)} \right], \quad (5)$$

where

$$F_{YP} = (-1)^{(|m|-m)/2} \sqrt{\frac{(2n+1)(n-|m|)!}{4\pi(n+|m|)!}}.$$

Applying the same derivation to the components E_r and E_θ, and adopting the notations used in Ref. 23, we obtain the expansion of the incident Gaussian beam on the lth sphere,

$${}^G E_l = \sum_{n=1}^{\infty} \sum_{m=-n}^{n} \sum_{p=1}^{2} {}^G C_{mnp}^l |mn1p\rangle,$$

where $|mnjp\rangle$ is the Dirac notation with $p=1$ for $\boldsymbol{M}_{mn}^{(j)}$ and $p=2$ for $\boldsymbol{N}_{nm}^{(j)}$. Here, ${}^G C_{mnp}^l$ for $p=1,2$ are

$${}^G C_{mn1}^l = E_0 \frac{-i^n(-1)^n(2n+1)}{n(n+1)F_{YP}} g_{nm,TE},$$

$${}^G C_{mn2}^l = E_0 \frac{i^{n-1}(-1)^n(2n+1)}{n(n+1)F_{YP}} g_{nm,TM}. \quad (6)$$

The scattered field is a sum of the scattered electric field from all the spheres,

$${}^S E = \sum_{l=1}^{\oplus L} {}^S E_l = \sum_{l=1}^{\oplus L} \sum_{n=1}^{\infty} \sum_{m=-n}^{n} \sum_{p=1}^{2} {}^S C_{mnp}^l |mn3p\rangle. \quad (7)$$

The symbol $\oplus$ means that the sum should be performed in the Cartesian coordinates. ${}^S C_{mnp}^l$ is the scattering expansion coefficients for the VHS $|mn3p\rangle$, which is calculated by the order-of-scattering method.[23,24] In this method, ${}^G C_{mn}^l$ and ${}^S C_{mnp}^l$ are written as the corresponding incident and scattering matrices for a system of L spheres: ${}^L \boldsymbol{G}_l$ and ${}^L \boldsymbol{T}_l$. Using the matrix $\Psi^{(L)}$ to represent the response of the L-sphere system, the relation between incident and scattering matrices is simply expressed as[24]

$$[{}^L T_1, {}^L T_2, {}^L T_3, \ldots, {}^L T_L] = [G_1, G_2, G_3, \ldots, G_L] \Psi^{(L)}. \quad (8)$$

For conciseness, we give $\Psi^{(L)}$ directly,

$$\Psi_{LL}^{(L)} = S_L \sum_{i=0}^{\text{Nos.}} (\Omega^{(L-1)} \Psi^{(L-1)} \Omega'^{(L-1)} S_L)^i,$$

$$\Psi_{pL}^{(L)} = \sum_{j=1}^{L-1} \Psi_{pj}^{(L-1)} \Omega_{j,L} \Psi_{LL}^{(L)}, \quad p = 1, \ldots, L-1,$$

$$\Psi_{Lq}^{(L)} = \Psi_{LL}^{(L)} \sum_{j=1}^{L-1} \Omega_{L,j} \Psi_{jq}^{(L-1)}, \quad q = 1, \ldots, L-1,$$

$$\Psi_{pq}^{(L)} = \Psi_{pq}^{(L-1)} + \Psi_{pL}^{(L)} \sum_{j=1}^{L-1} \Omega_{L,j} \Psi_{jq}^{(L-1)}, \quad p,q = 1, \ldots, L-1, \quad (9)$$

where $\Omega^{(L-1)} = [\Omega_{L,1}, \Omega_{L,2}, \ldots, \Omega_{L,L-1}]$ and $\Omega'^{(L-1)} = [\Omega_{L,1}, \Omega_{L,2}, \ldots, \Omega_{L,L-1}]^T$. Here, $\Omega_{k,l}$, obtained from the addition theorem,[27] is the translation matrix from a coordinate system centered on the kth sphere to a coordinate system centered on the lth sphere.

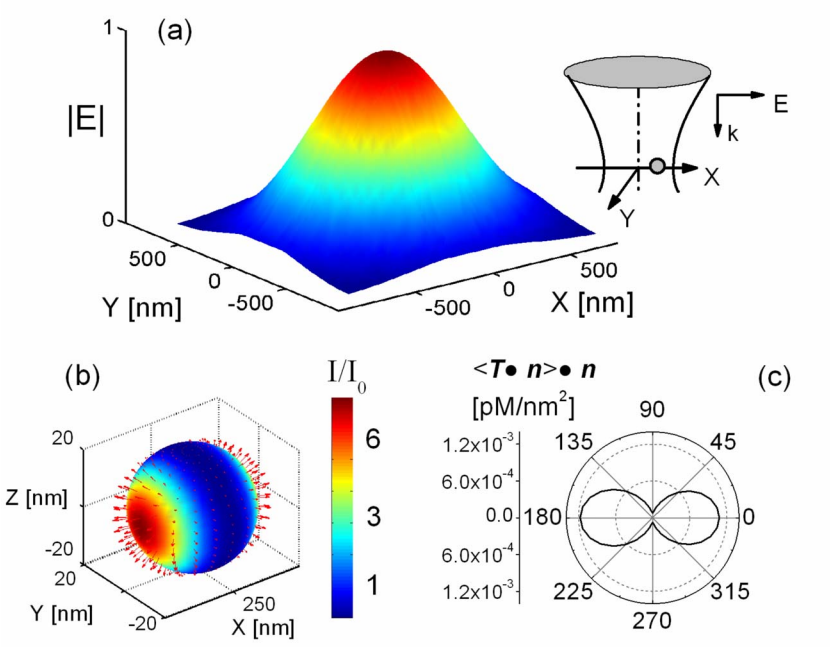

FIG. 1. (Color online) (a) Field profile of the Gaussian beam in focal plane for $\lambda=830$ nm and $w_0=500$ nm. The geometry of the 2D optical trapping is shown in the inset. (b) The optical pressure distribution over the surface of a silver sphere ($R=20$ nm) positioned at $w_0/2$ along x axis for an incident power $P=50$ mW. The colors represent the light intensity. (c) The pressure component along the surface normal around the equator of the sphere in the focal plane.

After knowing the scattering electric field, the magnetic field can be obtained through the relations

$$H=\frac{1}{i\omega\mu}\nabla\times E,\quad N=\frac{1}{k}\nabla\times M,\quad M=\frac{1}{k}\nabla\times N. \quad (10)$$

The time-averaged optical force acting on a nanosphere is finally calculated by integrating the Maxwell stress tensor $T_{ij}=\varepsilon E_iE_j+1/\mu B_iB_j-1/2(\varepsilon E^2+1/\mu B^2)\delta_{ij}$ over the surface S of the sphere,[25]

$$\langle F\rangle=\oint_S\langle Tn\rangle ds. \quad (11)$$

The optical potential is then the work needed to move the particle from position r_0 to infinity,

$$U=-\int_\infty^{r_0}\mathbf{F}(\mathbf{r})\cdot d\mathbf{r}. \quad (12)$$

III. RESULTS AND DISCUSSIONS

In the following, we will illustrate the simulation technique described above through examples that may have experimental relevance. We confine our study to Au and Ag spheres with radii between 20 and 100 nm, thus including the size range for which colloidal particles can be readily synthesized. Further, we restrict ourselves to optical forces and interactions in the focal plane of a focused laser beam, thus simulating the case when the movement of particles along the optical axis of the optical tweezers is restricted by a substrate.[17] We first illustrate the case of one trapped particle and then go on to the more interesting case of two interacting particles, where one of the particles is fixed at a certain distance from the beam center and the other particle is free to move in response to the total optical potential in the focal plane.

Figure 1(a) shows the spatial distribution of the electric field modulus of a Gaussian beam centered at the z axis (wavelength $\lambda=830$ nm and beam waist radius $w_0=500$ nm) in the focal plane ($z=0$) obtained by the "on-axis" VSH expansion.[21] The multipole order n is here truncated at $N=12$. The relative error for both the modulus and the phase angle of the electric field is less than 10^{-3} compared to the Davis formula[20] (not shown), which is enough for the convergence and accuracy of the calculation. For the "off-axis" case,[22] i.e., for the case when the particles are not on z axis, the accuracy becomes lower. Considering that the Gaussian beam is in itself an approximation to a tightly focused beam in an experiment, the off-axis VSH expansion should still be meaningful for estimating a wide range of trapping effects.

Optical trapping of a single silver nanoparticle by a Gaussian beam is illustrated in the inset of Fig. 1(a). A Ag sphere with a radius $R=20$ nm is placed at the position $x=w_0/2$, $y=z=0$. Figure 1(b) illustrates the pressures exerted on different parts of the surface of the sphere by red arrows, while the light intensity distribution over the surface is illustrated by the color bar. The net force is obtained by integrating the pressure over the whole surface. In a plane wave, the net force in any direction perpendicular to the incident k-vector would be zero. In the Gaussian beam, however, the incident light intensity varies in the xy plane, which results in a net optical force pointing toward the beam center. Figure 1(c) shows the pressure component along the surface normal around the sphere's equator in the focal plane. An asymmetric pressure distribution is clearly seen, as expected from the induced dipole moment in the particle. As shown in Fig. 2, the transverse optical force goes to zero when the sphere is moved to the beam center, where the optical potential is minimum. In order to trap the Ag nanoparticle at the center of the beam, the potential depth has to surpass the thermal kinetic energy of the nanoparticle ($\sim 1k_BT$). For the present set of parameters, this is clearly the case.

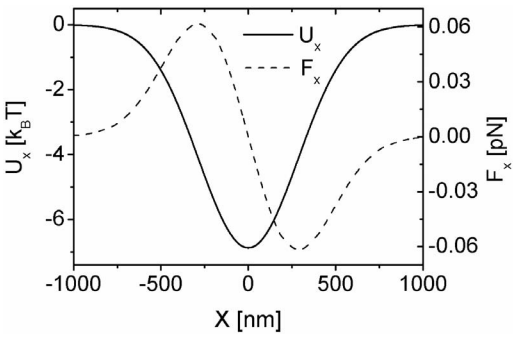

FIG. 2. The transverse optical force (dashed line) and the optical potential (solid line) experienced by a silver nanoparticle (R =20 nm) in water for the case when the particle is situated in the focal plane of a x-axis polarized Gaussian beam (λ=830 nm, w_0 =500 nm, P=50 mW). The potential is expressed in units of k_BT, where T=300 K.

In the experiment of Ref. 17, a silver nanoparticle is trapped in two dimensions by a focused laser beam of wavelength λ=830 nm. The optically trapped particle is then moved close to an immobilized nanoparticle, stuck on the cover glass substrate, to create "hot" particle dimers for SERS. Our previous calculations showed that dimers should form when the particle-particle distance is less than approximately half the beam waist. Here, we give more detailed results and discussions about this two-sphere interaction for different particle sizes and for different incident wavelengths. We also make a comparison to the van der Waals forces that exist between the particles in the absence of any external illumination.

As shown in the inset of Fig. 3(a), the Gaussian beam is centered on the origin of the coordinate system. An immobilized particle "I" is placed on the positive x axis at a distance D from the origin. We now calculate the optical potential experienced by a particle "F," which is free to move along the x axis, as a function of x for different values of D. We first restrict ourselves to two incident wavelengths (λ =514.5 nm and λ=830 nm), to the case of homodimers, i.e., $R_1=R_2=R$, and to the case when the polarization of the Gaussian beam is along the x axis. When the beam center is far away from the origin (D=600 nm, dashed lines), only a small part of the incident light actually hits the immobilized particle. The optical potential is then similar to the case of a single particle in Gaussian beam. It is clear that for a proper incident power, the movable nanoparticle can be trapped in the beam center. For example, for a Ag sphere with R =20 nm, at λ=514 nm and for P=10 mW, the trapping potential $|U|=2.5k_BT$, and at λ=830 nm and P=20 mW, $|U|$ $=2.4k_BT$. However, it is unlikely that a nanoparticle that is initially trapped at the center of the Gaussian beam will overcome the relative large potential barrier toward the immobilized particle to form a dimer. When D=250 nm (thick solid lines), the potential barrier between the beam center and the origin has decreased considerably, and in some cases, the potential curve is so distorted that the original Gaussian potential well cannot be distinguished. In general, a Ag nanoparticle trapped at the beam center then has the possibility to overcome the barrier to form a particle pair. An exception is

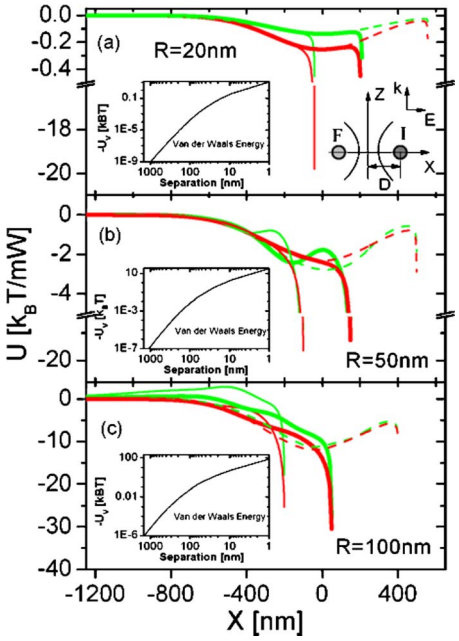

FIG. 3. (Color online) The optical potential experienced by a mobile silver particle (F) close to an identical immobilized particle (I) as a function of the x position of the mobile particle. The right inset in (a) shows the optical trapping configuration for the two-particle system. The radii of spheres are R=20, 50, and 100 nm for (a)–(c), respectively. Different separations, D=0, 250, and 600 nm, between the beam focus and the position of the immobilized particle are represented by dashed, thick solid, and thin solid lines (green for λ=514 nm and red for λ=830 nm), respectively. The surrounding medium is water and T=300 K. The insets to the left in (a)–(c) are the corresponding van der Waals energies of two silver spheres as a function of the surface separation.

the case of R=50 nm at λ=514 nm shown in Fig. 3(b), where the barrier is considerable (thick green line). It is difficult for the nanoparticle F to overcome the barrier under an incident laser power $P>3$ mW. Even when the beam center moves to the origin (thin green line), the barrier is still about $2.3k_BT$ for an incident power P=20 mW.

The case of Au particles is shown in Fig. 4. The configuration is the same as that in the inset of Fig. 3(a). The potential of the particle at the beam center is the lowest at λ =633 nm (red lines) for all cases, R=20, 50, and 100 nm; i.e., it is possible to trap the gold particle with the 633 nm Gaussian beam. As the distance D decreases, nanoparticle pairs can eventually form, just as in the case of Ag above. However, when the incident wavelength λ=514 nm, i.e., close to the particle plasmon resonance wavelength, the real part of the polarizability is negative for R=50 and 100 nm Au spheres. This is because of the strong surface plasmon shift induced by retardation effect for large particles. The gradient force thus turns out to be repulsive and optical trapping becomes impossible. Hence, the potential exhibits a maximum at the beam center, as shown in Figs. 4(b) and 4(c).

For closely spaced nanoparticles, the van der Waals force cannot be neglected. To illustrate this effect, we have plotted the van der Waals interaction energy U_v for the two nanopar-

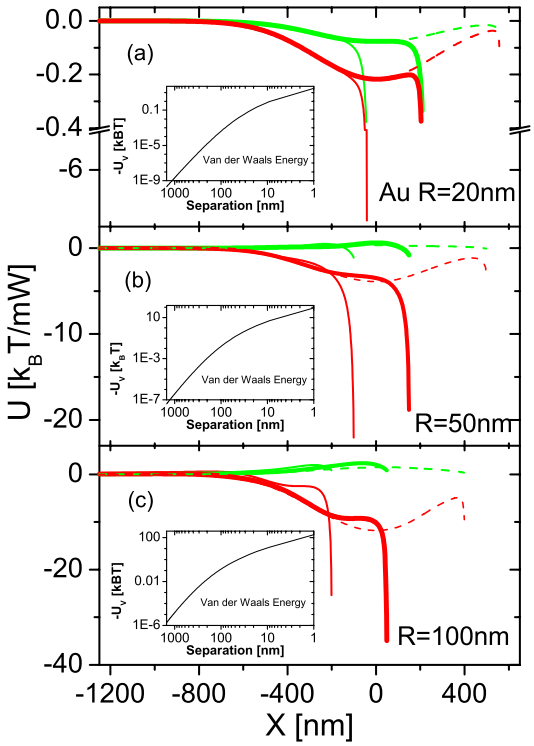

FIG. 4. (Color online) Identical plots as in Fig. 3 but for Au particles.

ticles in the insets of Figs. 3 and 4. The plots show that the van der Waals force is small compared to the optical forces for separations $d>10$ nm and for an incident power $P=10$ mW. However, when the separation decreases further, the van der Waals force increases dramatically and at $d=1$ nm and $R=20$ nm, U_v is about $-11k_BT$ for the Ag particle pair, which is enough to bond the nanoparticle pairs tightly without the assistance of optical forces. This result is expected, considering that the van der Waals energy is proportional to the inverse sixth power of the particle separation. One may note that for most stable colloidal nanoparticle systems, one would also need to take into account Coulomb repulsion due to surface charges on the nanoparticles, which may prohibit actual contact between the particles.

The potential barrier close to the origin, shown by the thick green curve in Fig. 3(b), is caused by the out-of-phase interaction of the induced dipoles in the nanoparticles. This effect is analogous to the interparticle optical potential obtained for a particle dimer illuminated by a plane wave, for which the different phases of the dipoles result in an oscillation of the optical potential as a function of the interparticle distance.[28] For a Gaussian beam, the oscillation can be more clearly seen if we subtract the potential of a single particle (U_s) from the potential of the two interacting particles, as shown in Fig. 5. It is obvious that the period of the oscillation is close to $\lambda/2$, which shows that the optical potential barrier seen in Fig. 3(b) is caused by an out-of-phase dipole interaction between the two metal nanoparticles.

Before the attractive optical force and the van der Waals force become dominant at very small separations, the repulsive optical force mentioned above could hinder the two

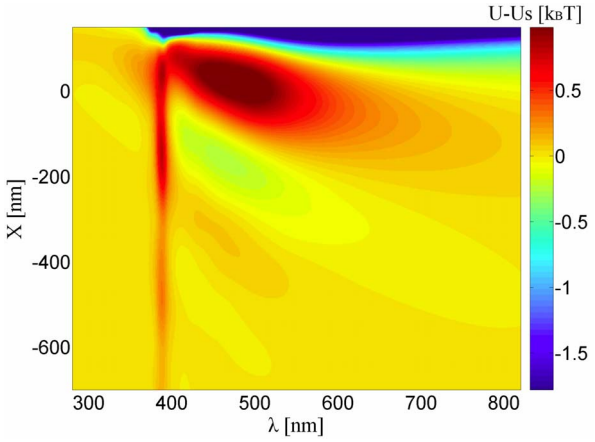

FIG. 5. (Color online) Pseudocolor plot of U-U_s (see text for description) for silver particles ($R=50$ nm) as a function of the x position of particle F and of the illumination wavelength. The immobilized sphere is situated on the x axis at a distance $D=250$ nm from the origin. The incident power of the Gaussian beam ($w_0=500$ nm) is 1 mW, the surrounding medium is water, and $T=300$ K.

nanoparticles from forming a pair. This effect is particularly pronounced when the wavelength of the Gaussian beam is close to the collective resonance wavelength of the nanoparticles. For specific illumination wavelengths, one may even expect a stable equilibrium distance between the nanoparticles.[29] Figure 6 shows the two-dimensional (2D) distribution of the optical force exerted on sphere F ($R=100$ nm) in the focal plane under resonant illumination ($\lambda=470$ nm) and a power of 10 mW. The filled circle represents the immobilized sphere I, which is situated on the x

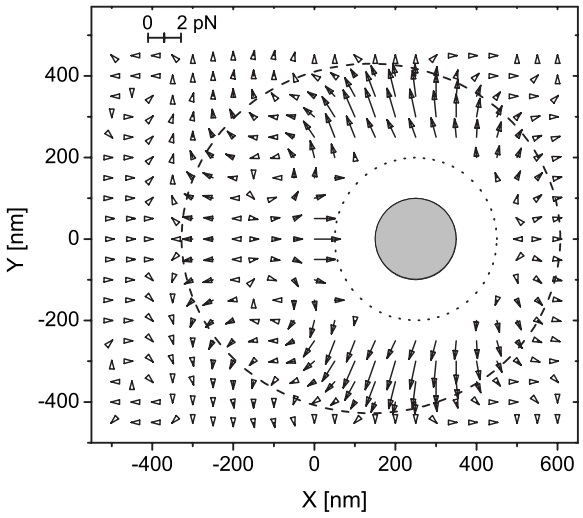

FIG. 6. Vector plot of the optical forces exerted on the Ag sphere F in the focal plane of a Gaussian beam ($w_0=500$ nm) for the case when the incident wavelength is close to the particle plasmon resonance. The immobilized sphere I is situated at $+x$ axis at $D=250$ nm (see right inset in Fig. 3). The radius of the spheres are 100 nm and the laser power is 10 mW. The surrounding medium is water.

axis at a distance to the origin of $D=250$ nm. The dotted circle represents the case when the mobile sphere F touches the immobilized sphere I. The arrows denote the direction and the magnitude of the optical force exerted on the sphere F. Along the x axis, the optical force is attractive at small distances, but the force turns repulsive after the sphere F passes $x \approx -200$ nm. The largest repulsive force along the x axis is 0.68 pN, which occurs when F is at $x=-317$ nm. The potential barrier in the x direction, caused by this repulsive force, is $21.8k_BT$ (not shown), which would clearly prevent F from forming a dimer with I. Actually, the repulsive forces at certain distances, indicated as the dashed circle, can be expected to completely block dimerization; i.e., there is no path with a low enough energy barrier accessible for F toward the potential well corresponding to touching particles. This illustrates the very complex particle dynamics that, in general, can be expected for plasmonic particle systems illuminated near resonance.

IV. LIMITATIONS

The localized beam model we used here is an approximation to the first-order Gaussian beam. The average error of the first-order Gaussian beam is $\sim 0.457\%$ for $s=0.1$ ($s=\lambda/2\pi w_0$) and $\sim 4.33\%$ for $s=0.3$.[30] For a tightly focused beam, as generated by a microscope objective with high numerical aperture, i.e., $s \sim 0.2$, the localized beam model gives rise to artifacts.[22] However, the main artifact is several microns away from the Gaussian focus, while our calculation is only related to the part of ~ 2 μm around the focus, as dictated by the radii of the nanoparticles and the relevant particle separation range. The results presented here are thus expected to be valid from a simulation point of view. However, quantitative comparison with experiments should be performed with caution, in particular, considering the deviations from perfect particle sphericity that is characteristic of colloidal nanoparticles. An extended treatment will also need to consider the case of dissimilar nanoparticles, i.e., heterodimers. Quantitative comparison with experiments may also involve corrections for chromatic and spherical aberrations in the illumination system, as discussed in Ref. 3, although such effects can probably be accounted for by utilizing an effective beam radius larger than the diffraction limit.

V. CONCLUSION

We have presented a method based on the generalized Mie theory that allows us to calculate the optical forces in aggregates of interacting metallic nanoparticles illuminated by a Gaussian beam. This method has the advantages that it includes both the effects of mutipoles and retardations, which is crucial for obtaining correct results at both large and small distances compared to the particle radius. Using this method, we investigated the optical forces that act on a pair of interacting plasmonic Au or Ag particles in a focused Gaussian laser beam. The results point to a rich particle dynamics, such as repulsion and attraction, at various distances determined by field retardation and the resonant properties of the nanoparticles.

ACKNOWLEDGMENTS

H.X. Xu acknowledges the financial support from NSFC (Grant No. 10625418), MOST (Grant No. 2006DFB02020), and the "Bairen" projects of CAS. We thank B. Sepúlveda for stimulating discussions.

*Corresponding author. hongxingxu@aphy.iphy.ac.cn

[1] A. Ashkin, J. M. Dziedzic, J. E. Bjorkholm, and S. Chu, Opt. Lett. **11**, 288 (1986).
[2] A. Ashkin, Proc. Natl. Acad. Sci. U.S.A. **94**, 4853 (1997).
[3] N. B. Viana, M. S. Rocha, O. N. Mesquita, A. Mazolli, P. A. MaiaNeto, and H. M. Nussenzveig, Phys. Rev. E **75**, 021914 (2007).
[4] Y. Harada and T. Asakura, Opt. Commun. **124**, 529 (1996).
[5] P. C. Chaumet and M. Nieto-Vesperinas, Opt. Lett. **25**, 1065 (2000).
[6] A. Ashkin, Biophys. J. **61**, 569 (1992).
[7] L. Novotny, R. X. Bian, and X. S. Xie, Phys. Rev. Lett. **79**, 645 (1997).
[8] F. V. Ignatovich and L. Novotny, Rev. Sci. Instrum. **74**, 5231 (2003).
[9] A. S. Zelenina, R. Quidant, and M. Nieto-Vesperinas, Opt. Lett. **32**, 1156 (2007).
[10] V. Wong and M. A. Ratner, Phys. Rev. B **73**, 075416 (2006).
[11] G. Volpe, R. Quidant, G. Badenes, and D. Petrov, Phys. Rev. Lett. **96**, 238101 (2006).
[12] H. X. Xu, E. J. Bjerneld, M. Käll, and L. Börjesson, Phys. Rev. Lett. **83**, 4357 (1999).
[13] A. J. Hallock, P. L. Redmond, and L. E. Brus, Proc. Natl. Acad. Sci. U.S.A. **102**, 1280 (2005).
[14] M. Moskovits, Rev. Mod. Phys. **57**, 783 (1985).
[15] H. X. Xu, J. Aizpurua, M. Käll, and P. Apell, Phys. Rev. E **62**, 4318 (2000).
[16] F. Svedberg and M. Käll, Faraday Discuss. **132**, 35 (2006).
[17] F. Svedberg, Z. P. Li, H. X. Xu, and M. Käll, Nano Lett. **6**, 2639 (2006).
[18] J. A. Stratton, *Electromagnetic Theory* (McGraw-Hill, New York, 1941).
[19] H. X. Xu and M. Kall, in *Surface-Enhanced Raman Scattering: Physics and Applications*, edited by K. Kneipp, M. Moskovits, and H. Kneipp (Springer, Berlin, 2006), Vol. 103, p. 87.
[20] L. W. Davis, Phys. Rev. A **19**, 1177 (1979).
[21] J. A. Lock and G. Gouesbet, J. Opt. Soc. Am. A **11**, 2503 (1994).
[22] G. Gouesbet and J. A. Lock, J. Opt. Soc. Am. A **11**, 2516 (1994).
[23] H. X. Xu, Phys. Lett. A **312**, 411 (2003).
[24] Z. P. Li and H. X. Xu, J. Quant. Spectrosc. Radiat. Transf. **103**, 394 (2007).
[25] J. D. Jackson, *Classical Electrodynamics* (Wiley, New York, 1998).
[26] G. Gouesbet, B. Maheu, and G. Gréhan, J. Opt. Soc. Am. A **5**, 1427 (1988).
[27] S. Stein, Q. Appl. Math. **19**, 15 (1961).
[28] H. X. Xu and M. Käll, Phys. Rev. Lett. **89**, 246802 (2002).
[29] B. Sepúlveda, J. Alegret, and M. Käll, Opt. Express **15**, 14914 (2007).
[30] J. P. Barton and D. R. Alexander, J. Appl. Phys. **66**, 2800 (1989).